Laser Assisted Brazing of Titanium to Aluminum Alloy

I. Tomashchuk*, P. Sallamand, M. Duband
Laboratoire Interdisciplinaire Carnot de Bourgogne, UMR 6303 CNRS - Université de Bourgogne-Franche-Comté, France
*Corresponding author: 12 rue de la Fonderie, 71200 Le Creusot, France, iryna.tomashchuk@u-bourgogne.fr

Abstract: Laser assisted brazing with Al-Si fillers in V-shaped groove configuration is a perspective method for joining of aluminum alloys to titanium. The quality of brazed interface is determined by Ti diffusion distance in the melted zone that becomes, after the solidification, a compact layer of Al-Ti-Si phases. Typical defect of this type of joints resides in lack of brazing at the bottom of the groove that becomes even more pronounced when thickness of materials overpasses 2 mm.
The present work introduces multiscale model that allows estimating diffusion process at titanium/melted zone interface in function of thermal history of welded plates. 3D model of heat transfer with moving laser source and fixed geometry is linked to 2D model of cross section of the groove where Fick equation is solved basing on the thermal history of a slice.
Comparison of maximal temperatures attained by the groove and Ti diffusion distances allowed concluding that for efficient brazing Ti side of the groove must reach 1200 K. Model allows estimating the effect of thermal field on diffusion distance of Ti in the melted zone and thus predicting the fraction of brazed surface of chamfer. Associated parametric studies help to understand the effect of joint geometry and heat source parameters on brazing efficiency and propose optimized operational condition.

Keywords: laser assisted brazing, dissimilar interfaces, titanium, aluminum alloys, heat transfer, diffusion.

1. Introduction

Joining of aluminum alloys to titanium alloys remains a difficult technological task because of important mismatch in physical properties, limited mutual solubility and formation of brittle intermetallic phases in aluminum-titanium (Al-Ti) system [1].

Promising results on aluminum-titanium laser joining were obtained by using brazing approach, when only aluminum side of the joint undergoes fusion and resulting tensile strength is related to thickness of intermetallic layer formed on titanium side. Chen et al. [2] studied laser assisted brazing in V-shaped groove configuration with Si-containing filler wire and reported beneficial effect of $Ti_7Al_5Si_{12}$ on depressing the growth of brittle Al_3Ti phase. According to the thermodynamic model proposed by Chen, Li, Chen et al. [3], the accumulation of Si near solid Ti interface strongly depends on local quantity of Ti migrated in liquid zone: minimal chemical potential is reached when molar fraction of Ti approaches 0.5. Chen, Chen & Li [4] demonstrated the influence of heat flow variation along solid Ti side on the morphology of resulting Si-containing microstructures. In this experiment, the groove was machined only at aluminum alloy side, while titanium interface remained perpendicular to the top surface of the plate. Gaussian laser beam has been modulated into rectangular spot having Gaussian distribution in cross-direction and uniform distribution along joint line. It was observed that while the top of the interface demonstrated well-advanced interfacial reactions, the bottom of the weld suffered from lack of energy and served a start-point of crack propagation during tensile tests. The uniform morphology of interfacial microstructures on solid Ti side was obtained by Chen, Li, Chen, Dai et al. [5] when 45° grooves from both titanium and aluminum sides were associated with modulated rectangular spot of same shape as mentioned above. According to the numerical model of heat transfer proposed by Chen, Li, Chen, Dai et al. [5], the use of rectangular spot allowed reducing the difference of temperatures attained in different parts of titanium side of the groove. UTS of 278 MPa has been achieved in this way, and fracture took place in the seam.

In all reported studies, thickness of the plates did not overpass 1.5 mm and joining is performed in one pass. Present research deals with joining of 3 mm thick titanium T40 and AA5754 alloy with use of Al-12Si filler. Gaussian laser spot is divided in two half-spots by optical blade and defocused in order to have

bigger irradiated surface. Numerous experiments showed that typical defect of this type of assemblies resides in lack of brazing at the bottom of the groove.

In order to understand the relation between experimental conditions and efficiency of brazing, a multiscale simulation that allows estimating diffusion process at titanium/melted zone interface in function of thermal history of welded plates is proposed. 3D model of heat transfer with moving laser source and fixed geometry is linked to 2D model of cross section of the groove where Fick equation is solved basing on the thermal history of a slice.

2. Mathematical model

2.2 Governing equations

Heat transfer problem is solved over domain having exact dimensions of welded plates (Figure 1): 200 x 100 x 3 mm plates with machined V-shaped chamfer.

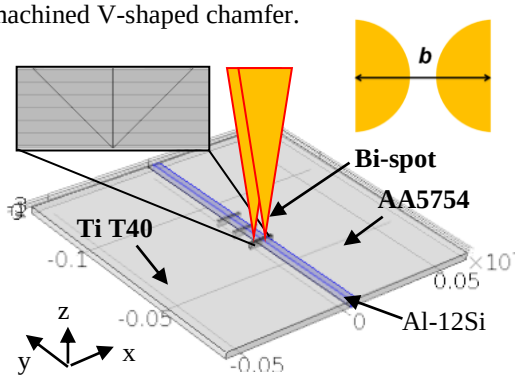

Figure 1. 3D model geometry and sketch of laser spot configuration.

Following simplifications were adopted in this study:

- defocused laser tandem is considered as surface heat source;
- convection and surface tension phenomena are neglected, the chamfer is assumed as filled with Al-12Si.

Average height of deposited Al-12Si material can be estimated from relation :

$$h_{Al-12Si}^{av} = D_{wire} \cdot \sqrt{\frac{\pi \cdot V_{wire}}{2 \cdot V_w \cdot \left[tg(\alpha_{AA5754}) + tg(\alpha_{T40})\right]}}$$

where V_{wire} – wire speed (m/s), V_w – linear laser speed (m/s), D_{wire} – wire diameter (mm), $cos(\alpha_{AA5754})$ and $cos(\alpha_{T40})$ – opening angles of chamfer from AA5754 (fixed to 45°) and Ti T40 sides.

Heat transfer equation is solved in time dependent form over 3D domain including welded plates and pre-filled chamfer:

$$\rho \cdot C_p \cdot \frac{\partial T}{\partial t} + \vec{\nabla}\left(-k\vec{\nabla}T\right) = 0$$

where ρ - volumetric mass (kg/m^3) and k – thermal conductivity (W·m^{-1}·K^{-1}) are given as functions of temperature in following form:

$A = A_{solid} + (A_{liquid} - A_{solid}) \bullet flc2hs(T - T_m, dT)$,

where *flc2hs* is smoothing Heaviside function, $T_m = T_{liquidus} - T_{solidus}$ is melting temperature and dT – smoothing interval.

Specific heat capacity C_p (J·kg^{-1}·K^{-1}) takes into account latent heat of fusion L_f:

$$C_p = C_p^{solid} + (C_p^{liquid} - C_p^{solid}) \cdot flc2hs(T - T_m, dT) + L_f \cdot \frac{\exp\left(-\frac{(T-T_m)^2}{(dT)^2}\right)}{\sqrt{\pi (dT)^2}}.$$

Defocused double spot laser is represented by a tandem of two half-spots with Gaussian distribution:

$$q_1 = \frac{a \cdot P}{2 \cdot \pi \cdot R^2} \exp\left(-\frac{(x - b/2)^2}{R^2} - \frac{(y + V_w \cdot t)^2}{R^2}\right) \cdot [x > -b/2]$$

$$q_2 = \frac{a \cdot P}{2 \cdot \pi \cdot R^2} \exp\left(-\frac{(x + b/2)^2}{R^2} - \frac{(y + V_w \cdot t)^2}{R^2}\right) \cdot [x < b/2]$$

where a – laser absorption coefficient, P – laser power (W), R – laser spot radius (m), b – distance between two half spots (Fig. 2), t – time (s).

Resulted thermal field is exported using linear extrusion tool into 2D model representing the transversal cut of the chamfer (Figure 2). To facilitate the post-treatment, 2D model is inclined at 45° (or more, depending on chamfer opening angle) in order to keep chamfer surface from Ti side parallel to axis z'.

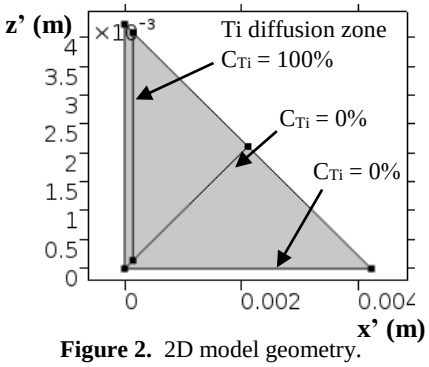

Figure 2. 2D model geometry.

Fick equation of Ti diffusion in the melted zone is solved over 2D domain:

$$\frac{\partial c_{Ti}}{\partial t} + \vec{\nabla}\left(-D_{Ti}\vec{\nabla}c_{Ti}\right) = 0$$

where

$$D_{Ti} = D_0 \cdot \exp\left(-\frac{E}{RT}\right).$$

Consistent stabilization was applied to both thermal and diffusion problems.

2.2 Boundary conditions

For 3D model, heat sources q_1+q_2 are applied at the top surface of plates and chamfer. Convective heat exchange with environment (h = 10 W/(m²·K)) is applied to all boundaries. Initial temperature of domain is of 300 K.

For 2D model, Ti fraction of 100 % (c = 1) is applied to the chamfer boundary representing Ti/melted zone interface. Fraction of 0 % (c = 0) is imposed as initial condition to the domain as well as boundary condition for second surface of the chamfer (Figure 2). Symmetry condition is applied to the top surface.

2.3 Solving and post-treatment

Time dependent segregated solver PARADISO was used. The problem was calculated over 15 s, with timestep of 0.1s.

Parametric solver was applied to investigate the effect of operational parameters on target functions defined below: Ti diffusion distance and % of brazed surface of the chamfer.

For the post-treatment analysis, maximal temperatures reached at the interface Ti/melted zone were collected.

Diffusion distances of Ti were evaluated as:

$$L^{\max}_{C_{Ti}\geq 0.01} = x'_{\max} \cdot (C_{Ti} \geq 0.01)$$

The zones of efficient brazing were identified as:

$$z'_B = \left(z'_{\max} - z'_{\min}\right) \cdot \left(L^{\max}_{C_{Ti}\geq 0.01} \geq 3 \cdot 10^{-6}\right).$$

This allows tracing diffusion map across Ti chamfer (Figure 3). The % of brazed surface can be determined as: $B(\%) = \frac{z'_B}{z'_{\max}} \cdot 100$.

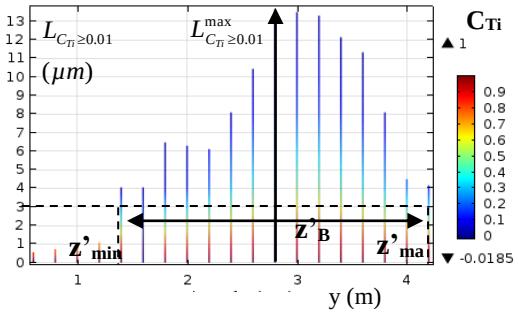

Figure 3. Example: diffusion map of Ti/MZ interface.

3. Results and discussion

3.1. Study of typical joining condition

To understand the relation between thermal history of Ti chamfer and its efficiently brazed surface, typical joining condition has been examined: laser power = 3.0 kW; linear laser speed = 0.55 m/min; beam defocusing from top surface = 8 mm (R = $1.78 \cdot 10^{-3}$ m); chamfer angle from both sides = 45°; thickness = 3 mm, gap between the spots b = 1.2 mm; heat source offset to Ti side = 0.9 mm, wire speed = 1.8 m/min.

Accordingly to calculated thermal field, at the interface between Ti T40 and melted zone (MZ) the temperature of Ti melting is not attained, in spite of high temperatures in zone of laser-matter interaction (Figure 4a). Thermal history of locations that correspond to different positions on z (z = 0 is the bottom of chamfer and z = 3 mm is the top) differs proportionally to their distance from heat source (Figure 4b). It is remarkable that maximal temperature is reached not at the top surface (z = 3 mm) but underneath (z = 2 mm).

The variation of maximal temperature of Ti/MZ interface with z compared with diffusion distances (Figure 5a) shows that diffusion interface starts to develop itself starting from temperature of 1150 K and becomes sufficiently thick (3 μm) for establishing mechanical continuity from 1200 K. Knowing that fusion temperature of Al-12Si is only of 850 K makes it clear that arrival of melted Al-12Si at Ti T40 surface does not always lead to efficient brazing.

To compare these results with experiment, X-map of Al content of MZ side of broken Ti/MZ interface was acquired (Figure 5b). Dark zones correspond to the surface depleted in Al and rich in Ti: here the break occurred within

diffusion interface where efficient brazing took place. Pink zones correspond to the places rich in Al and not containing Ti: here liquid Al-12Si was too cold to produce efficient brazing (T<1150 K). It can be seen that the propagation of brazed zone is not constant: periodical arrivals of hot wire down to the bottom of the interface also contribute to the development of brazing zones.

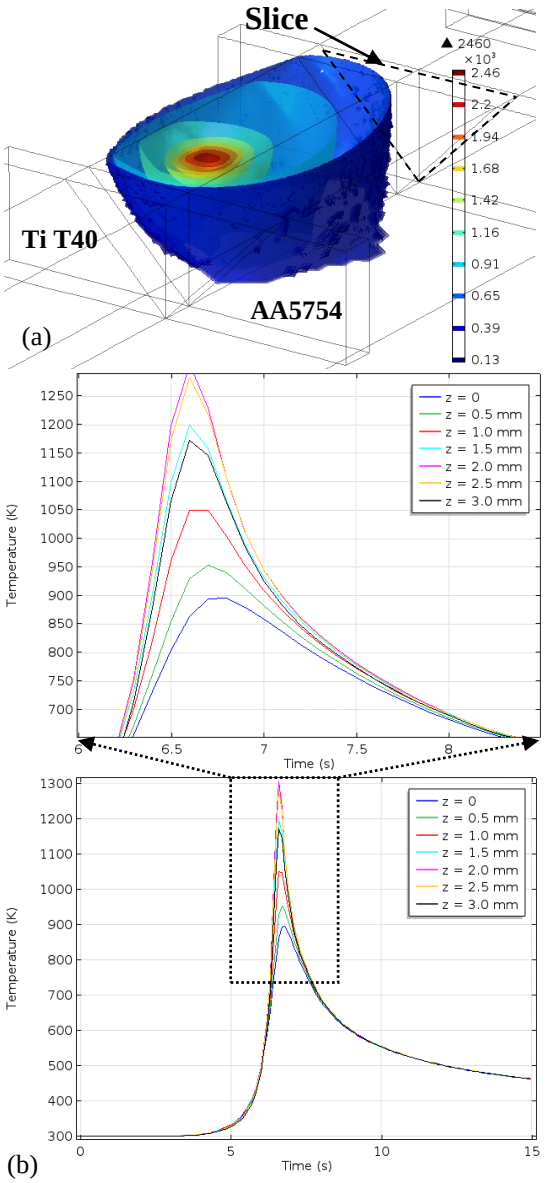

Figure 4. Thermal field (a) and thermal history of Ti/MZ interface slice at different z (b).

This simulation does not take into account fluid flow within the chamfer that is about to be filled, so the simulation estimates only brazed surface related directly with conductive heat transfer and neglects convective one. For this weld, zone of continuous brazing at Ti/MZ interface represents 58 % of chamfer surface, when calculation gives 57 %.

The measurement of total surface of "dark" and "pink" zones allows estimating global brazed surface around 80%, which means, convective heat transfer is responsible to about 20% of real brazed surface. However, purely conductive simulation allows estimation of "safety zone" where brazing interface will be continuous.

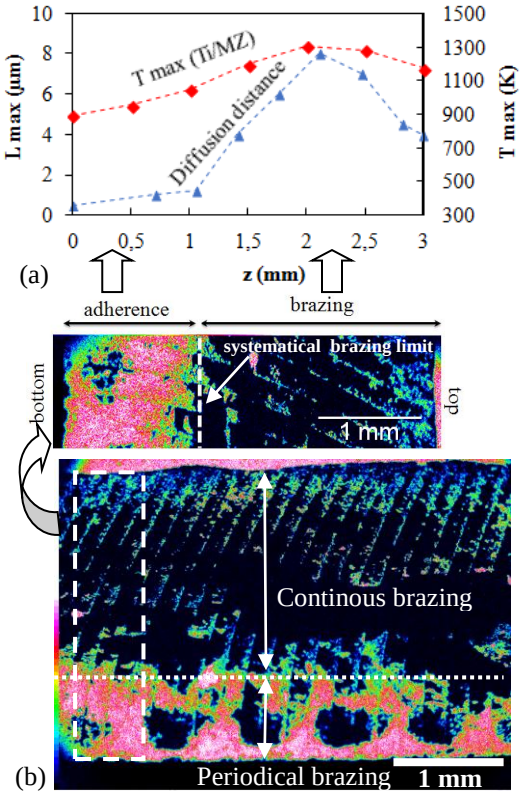

Figure 5. Diffusion distances and maximal temperatures attained by Ti/MZ interface (a); Al X-map of broken Ti/MZ interface (b).

Transversal cut of the weld undergone SEM-EDS analysis to determine the experimental distances of Ti diffusion in the melted zone. Comparison of experimental and calculated

diffusion distances at different z (Figure 6a,b) showed that:

- at the hottest zone of Ti/MZ interface diffusion distances are overestimated ($\Delta L \approx 2$ µm) because of neglection of convective heat transfer;
- at middle-height (z=1.5 mm) good concordance between calculated and observed diffusion profiles is observed.

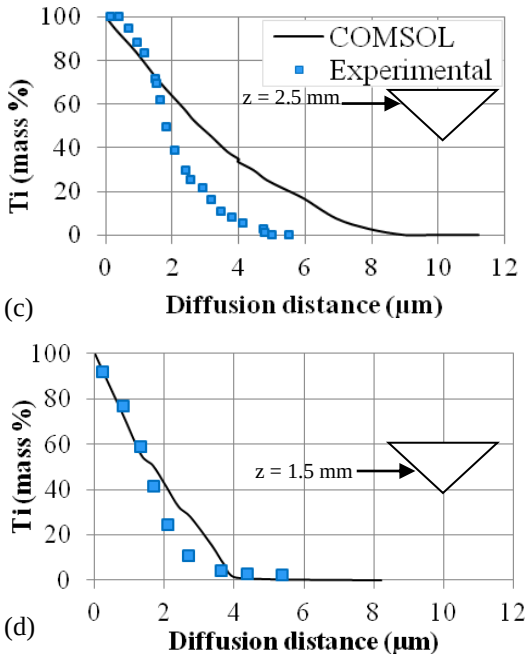

Figure 6. Ti diffusion profiles calculated at the top (c) and middle (d) of Ti/MZ interface.

3.2. Effect of operational parameters on brazing efficiency

Ideal condition for brazed interface can be formulated as follows:

- brazed interface should be maximized (T>1200 K);
- diffusion length should be ≥ 3 µm but must not exceed 20 µm because of risk of embrittlement.

To investigate the effect of different operational parameters on brazing efficiency, two groups of parametric calculations were performed:

- geometry effect estimation (the influence of chamfer angle and plate thickness);
- heat source effect estimation (influence of laser power, linear laser speed, bi-spot gap, laser offset from joint line and laser spot size).

While variating one parameter at once, all others are kept constant as in 3.1. The effect of every parameter within the window of considered values was estimated as *max-min* (Table 1).

It was found that geometry of the plates (thickness and opening chamfer angle at Ti T40 side, Figure 7) has the strongest influence on diffusion length and brazed surface. Even slight variation of plate thickness modifies completely thermal history of Ti/MZ interface. Simple reducing of plate thickness risks to create thick diffusion interfaces and embrittle the joint. Chamfer opening angle has strong influence on diffusion distance of Ti: as angle diminishes, heat source founds itself more and more close to Ti/MZ interface, provoking development of thick reaction layers at the top of Ti chamfer. However, only by varying opening angle, it seems impossible to attain 100% brazed surface. 45-50° opening angle allows at once to keep thin diffusion distances and maintain maximal brazed surface (about 60 %).

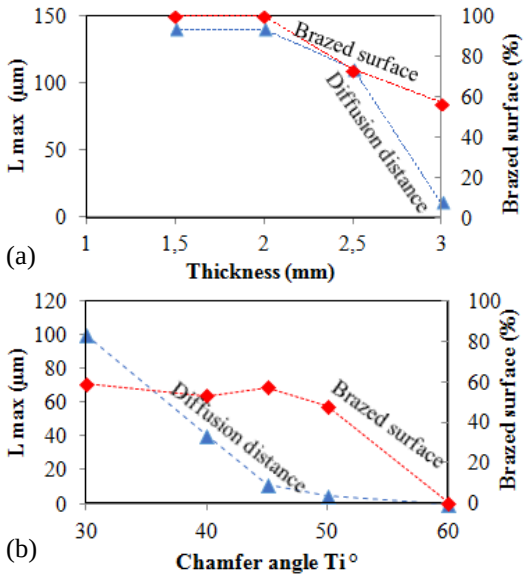

Figure 7. Evolution of diffusion distances and brazed surface % in function of joint geometry: plate thickness (a) and opening angle of Ti side chamfer (b).

Increase of laser power (Figure 8a) naturally has strong influence on the development of both brazed interface and diffusion length. However, the achievement of 100% brazing is related to the risk of embrittlement as diffusion lengths at the top of Ti/MZ interface overpass 100 µm. To keep diffusion distances below 20 µm, laser power must be limited to 3400 W, but brazed surface in this case will not overpass 80%.

Increase of linear laser speed (Figure 8b) leads to decrease of diffusion distances and brazed interface. The range of 0.45-0.55 m/min is the best compromise allowing keeping brazed surface at 70-50%.

The gap between two laser spots (Figure 1) has almost no influence on both diffusion distance and brazed surface (Figure 8c).

Beam defocusing (counted from top surface of the plates upwards) that controls the size of laser spots also makes no influence on brazing interface (Figure 8d). By focusing or defocusing laser beam it is possible to influence the diffusion distances alone, that can be interesting tool.

Offset of heat source from joint line towards Ti side makes no important influence on brazed surface (Figure 8e). However, it should not overpass 1100 µm to avoid the risk to create thick diffusion layers at the top of Ti/MZ interface.

The estimation of effect of various parameters on target functions (Table 1) represents the first step towards optimization study. In can be concluded that brazed surface and diffusion distance are both strongly influenced by plate thickness and opening angle.

Table 1: Effect of plates geometry and heat source parameters on variation of diffusion distance and brazed surface.

		Effect *max-min*	
Parameter	**Amplitude**	**L max (µm)**	**B (%)**
Laser power (W)	3000-4000	92	43
Laser speed (m/min)	0.35-0.65	50	48
Bi-spot gap (mm)	0.4-1.4	3	0
Beam offset (µm)	400-1400	66	14
Defocusing (mm)	0-12	12	5
Thickness (mm)	1.5-3	132	99
Chamfer angle (°)	30-60	100	59

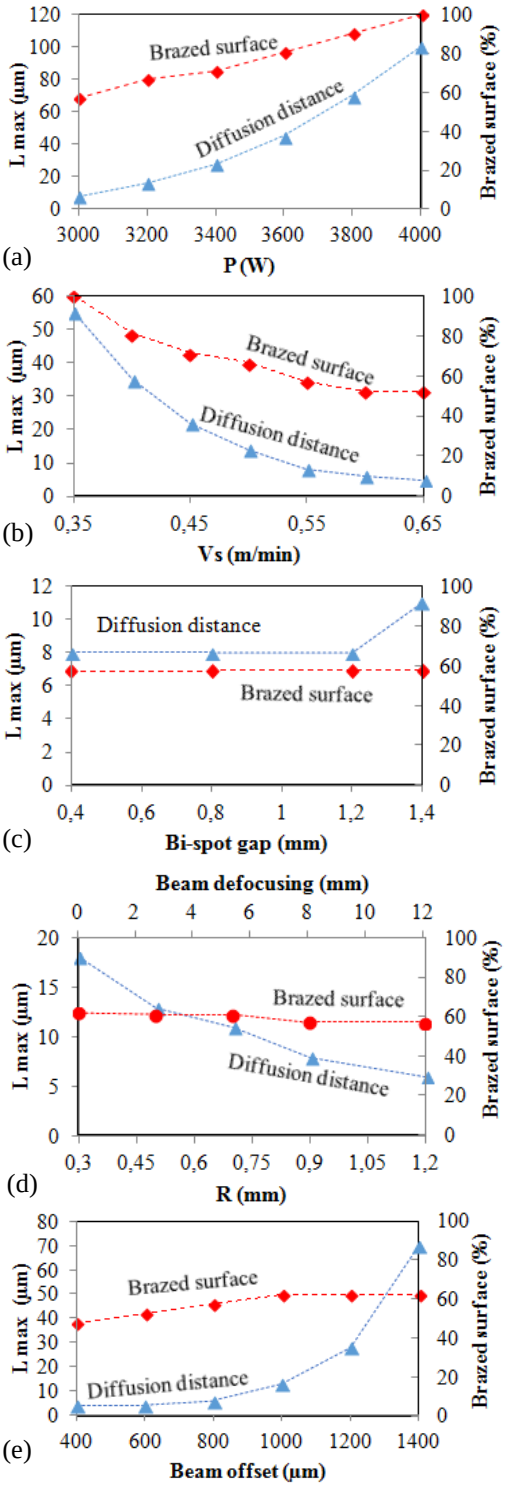

Figure 8. Evolution of diffusion distances and brazed surface % in function of heat source parameters: laser power (a), linear laser speed (b), gap between the spots (c), beam defocusing (d) and beam offset from joint line to Ti side (e).

Heat source parameters such as gap between laser spots and defocusing have weak influence and can be maintained on the levels established during preliminary experimental study (defocusing of 8 mm, b = 1.2 mm). Laser power, speed and offset from joint line have average effect on target functions but do not allow attaining 100% brazed interface.

3.3. Evaluation of two-pass joining

As parametric study indicates big difficulties to attain sufficient diffusion distance at the bottom of the groove, the feasibility of two-pass joining was tested. The first pass fills the chamfer at 1.5 mm of height (V_{wire} = 0.62 m/min), and second – up to 3 mm (V_{wire} = 1.85 m/min). Heat source parameters for the second pass are conserved the same as in 3.1, when the parameters for first pass were optimized through parametric study. Brazing condition for the first pass is estimated with present multiphysical model: laser power 2.3 kW; linear laser speed: 0.55 m/min; beam defocusing from top surface: 6.5 mm ($R = 1.78 \cdot 10^{-3}$ m); gap between the spots (b) = 1.2 mm; heat source centered at joint line, wire speed 1 m/min.

As illustrates Figure 9, first pass contributes to the development of diffusion interface between z = 0 – 1.5 mm, with maximal length of 8 µm. The second pass contributes to the development of diffusion interface between z = 1 – 3 mm. The middle height of the chamfer beneficiates the contribution of both passes, and superposition of two passes creates the zone of maximal diffusion distance around z = 1.5 mm. However, accurate choice of operational parameters allows avoid developing of thick diffusion zone in this location.

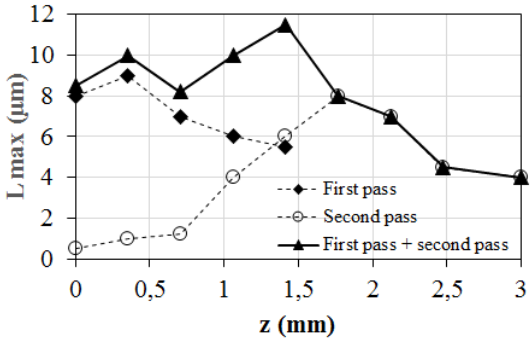

Figure 9. Calculated diffusion distances of standalone first and second passes and their common effect.

5. Conclusion

Present multiphysical and multiscale model allows estimation of brazing efficiency in V-shaped groove configuration.

Comparison of maximal temperatures attained by Ti/MZ interface and Ti diffusion distances allowed concluding that for efficient brazing Ti side of the groove must attain 1200 K.

Parametric study allowed estimating the influence of operational and geometrical parameters on brazed surface. It can be concluded that during one-pass filling of 3 mm thick V-shaped groove is impossible to attain uniform brazing on all surface of Ti/MZ interface by varying chamfer opening angle or heat source parameters. Accordingly to the model, it is possible to perform successful brazing in two passes, by filling 1.5 mm height each time. The condition allowing to conserve acceptable diffusion length (4-12 µm) and 100% brazed surface has been defined.

6. Acknowledgement

This work was supported by the French program Institut CARNOT Arts in the frame of the project ATTILA.

6. References

1. Raghavan, V., Aluminum-Titanium, *J. of Phase Equilib. and Diff.*, **26**, 171-172 (2005)
2. Chen, S., Li, L., Chen, Y., Dai, J., Huang, J., Improving interfacial reaction nonhomogeneity during laser welding-brazing aluminum to titanium, *Mater. Design*, **32**, 4408-4416 (2011)
3. Chen S., Li L., Chen Y., Liu D., Si diffusion behavior during laser welding-brazing of Al alloy and Ti alloy with Al-12Si filler wire, *Nonferrous Met. Soc. China*, **20**, 64-70 (2010)
4. Chen Y., Chen S., Li. L., Influence of interfacial reaction layer morphologies on crack initiation and propagation in Ti/Al joint by laser welding-brazing, *Mat. Design*, **31**, 227-233 (2010)
5. Chen S., Li L., Chen Y., Dai J., Huang J., Improving interfacial reaction nonhomogeniety during laser welding-brazing aluminum to titanium, *Mat. Design*, **32**, 4408-4416 (2011)